Spin-Polarized Structural, Electronic, and Magnetic Properties of Diluted Magnetic Semiconductors $Cd_{1-x}Mn_xS$ and $Cd_{1-x}Mn_xSe$ in Zinc Blende Phase

S. Nazir, N. Ikram, and M. Tanveer

Centre for Solid State Physics, University of the Punjab, Quaid-e-Azam Campus, Lahore 54590, Pakistan

A. Shaukat and Y. Saeed

Department of Physics, GC University, Faisalabad 38000, Pakistan

Ali Hussain Reshak*

Institute of Physical Biology-South Bohemia University, Nove Hrady 37333, Czech Republic

Received: January 19, 2009; Revised Manuscript Received: March 13, 2009

We studied the structural, spin-polarized electronic band structures, density of states, and magnetic properties of the diluted magnetic semiconductors (DMSs) $Cd_{1-x}Mn_xS$ and $Cd_{1-x}Mn_xSe$ in zinc blende phase (B3) with 25% Mn by using the ab initio method. The calculations were performed by using the full potential linearized augmented plane wave plus local orbitals (FP-L/APW+lo) method within the spin-polarized density functional theory and the local spin density approximation (LSDA). Calculated electronic band structures and the density of states of these DMSs are discussed in terms of the contribution of Mn $3d^54s^2$, Cd $4d^{10}5s^2$, S $3s^23p^4$, and Se $4s^24p^4$ partial density of states and we also compute the local magnetic moments. We estimated the spin-exchange splitting energies, Δ_x(d) and Δ_x(p−d), produced by the Mn 3d states, and we found that the effective potential for the minority spin is more attractive than that for the majority spin. We determine the s−d exchange constant $N_0\alpha$ and p−d exchange constant $N_0\beta$, which resembles a typical magneto-optical experiment. The calculated total magnetic moment is found to be 5.0020 and 5.00013 μ_B for $Cd_{1-x}Mn_xS$ and $Cd_{1-x}Mn_xSe$, respectively. These values indicate that every Mn impurity adds no hole carriers to the perfect CdS and CdSe crystals. Moreover, we found that p−d hybridization reduces the local magnetic moment of Mn from its free space charge value of $5.0\mu_B$ and produces small local magnetic moments on the nonmagnetic Cd and S sites.

Introduction

In diluted magnetic semiconductors (DMSs) the lattice is made up in part of substitutional magnetic atoms. The most extensively studied materials of this type are the $A^{II}{}_{1-x}Mn_xB^{VI}$ alloys, which are direct band gap semiconductors with a fraction of group II atoms replaced at random by Mn.[1,2] Mn has the electronic configuration $3d^54s^2$, where the 3d band is half-filled and has the ground-state configuration is $^6S_{(5)/(2)}$. The ternary nature of $A^{II}{}_{1-x}Mn_xB^{VI}$ gives us the possibility of tuning the lattice constant and band parameters by varying the composition of the material. The random distribution of magnetic ions over the cation sublattice leads to important magnetic effects, e.g., the formation of the spin-glass-like phase at low temperatures. The substitutional Mn atoms in the $A^{II}B^{VI}$ lattice are also characterized by highly efficient electroluminescence, which makes dilute $A^{II}{}_{1-x}Mn_xB^{VI}$ alloys important in the context of optical flat panel display applications. Furthermore, the presence of localized magnetic ions in these semiconductors leads to an exchange interaction between the sp band electrons and the d electrons associated with Mn^{2+}, resulting in extremely large Zeeman splittings of electronic levels.[3] A new class of materials, which have specific properties for the semiconductors, is formed with diluted magnetic semiconductors. DMSs have attracted tremendous interest because of the possibility of making quantum computing architecture using spin-polarized electrons localized in quantum dots as quantum bits.[4] DMSs have opened up vast experimental studies due to the possibility of electrical spin injection with efficiency up to 90% with n-type II−VI DMSs and several percent with p-type III−V DMSs.[5,6] Recently, it has become possible to control the magnetic state in InAs- or GaAs-based DMSs by light irradiation or an external electric field, and they are expected to be one of the basic components of spintronics devices.[7,8]

It is necessary to find materials that show ferromagnetism at a temperature as high as possible for device applications. Dietl et al. predicted that wide band gap DMSs materials such as GaMnN and ZnMnO would have a Curie temperature T_c above room temperature and also suggested that T_c values above 300 K could be achieved in $Ga_{0.9}Mn_{0.1}As$.[9] Particularly, Mn-based II−VI DMSs are stable in the antiferromagnetic phase; consequently, it becomes necessary to make a codoping by p-type carrier-induced ferromagnetism. The ferromagnetic ordering was observed in *p*-ZnMnTe at 1.5 K for $p = 1.2 \times 10^{20}$ cm^{-3}.[10] In current years resonant-photoemission measurements on $Cd_{1-x}Mn_xS$ and $Cd_{1-x}Mn_xTe$ have resolved some controversies about the experimentally assumed partial Mn 3d density of states (DOS).[11,12] The variation in the relative intensities of these Mn 3d features by changing the anion in a compound series, like $Cd_{1-x}Mn_xY$ or $Zn_{1-x}Mn_xY$ (Y = S, Se, Te), is promising to clarify the amount of p−d hybridization in these alloys.[13] Such a systematic study was reported for $Cd_{1-x}MnY$ by M. Taniguchi et al.[11] and for $Zn_{1-x}MnY$ by R. Weidemann et al.[14]

* To whom correspondence should be addressed. Phone +420 777729583. Fax. +420-386 361231. E-mail:maalidph@yahoo.co.uk.

10.1021/jp900698q CCC: $40.75
Published on Web 04/28/2009

CdMnS and CdMnSe DMSs have attracted great attention as they allow tuning the energy gap, the effective mass, and the lattice constant by varying the concentration of the Mn magnetic atoms. The experimental study of $Cd_{1-x}Mn_xS$ shows that it is distinguishable from other DMSs because of its significantly large p−d exchange integral value that causes various anomalous experimentally observed phenomena.[15] Further, CdMnS thin films have novel magnetic and magneto-optical properties caused by the hybridization between the Mn 3d and sp-hexagonal CdS.[16] Similarly, $Cd_{1-x}Mn_xSe$ diluted semiconductors have an interesting combination of magnetic and semiconducting properties which are used in many devices such as solar cells, gas sensors, etc. Therefore, a series of thin film of $Cd_{1-x}Mn_xSe$ ($0 \leq x \leq 0.5$) is fused onto precleaned amorphous glass substrate using a solution growth technique.[17] Such diluted Mn-doped semiconductors are of particular interest due to the spintronic effect.[18]

In CdMnS and CdMnSe, Cd has 4d and Mn has 3d valence electrons, and in DMSs the valence electrons of magnetic atoms in the d state play an important role. The analysis of valence band structure provides us essential information regarding the magnetic and transport properties of the diluted magnetic semiconductors. In this paper, we studied band structures and total and partial DOS with Mn 3d treated as valence states of $Cd_{1-x}Mn_xS$ and $Cd_{1-x}Mn_xSe$ DMSs using the full potential linearized augmented plane wave plus local orbitals (FP-L/APW+lo) method with local spin density approximation (LSDA) in order to understand the electronic-magneto properties of $Cd_{1-x}Mn_xS$ and $Cd_{1-x}Mn_xSe$ in the B3 phase with 25% Mn. The APW+lo basis set is used inside the atomic spheres for the Mn (3d) and Cd (4d) orbitals which are difficult to converge, while the LAPW basis set is used for all other partial waves.

Computational Methods

The calculations for structural, electronic, and magnetic properties of DMSs, $Cd_{1-x}Mn_xS$ and $Cd_{1-x}Mn_xSe$ in the B3 phase with 25% Mn, were performed within the framework of spin-polarized density functional theory. Particularly, we use the full potential linearized augmented plane wave plus local orbitals (FP-L/APW+lo) method as implemented in the WIEN2K package.[19] The electronic exchange-correlation energy is described by LSDA. Spin-polarized calculations are carried out with both spin-up and spin-down densities, and the corresponding two sets of Kohn−Sham single-particle equations are solved self-consistently. In the present self-consistent calculations, a muffin-tin model for the crystal potential is assumed and the unit cell is divided into two regions, within and outside the muffin-tin sphere. The electrons are paired into two groups, namely, the core electrons whose charge densities are confined within the muffin-tin spheres and the valence electrons. By solving the Dirac equation, we employ the fully relativistic effects for core states and use the nonrelativistic approximation for the valence states.

In these calculations, the FP-L/APW+lo basis set consists of the $3d^5 4s^2$ states of Mn, $4d^{10} 5s^2$ states of Cd, $4s^2 3p^4$ states of S, and $4s^2 4p^4$ states of Se. In both regions of the unit cell, different basis sets are used to expand the wave function, charge density, and potential. Inside the nonoverlapping spheres of muffin-tin radius R_{MT}, the linear combination of radial solution of the Schrödinger equation times the spherical harmonics is used, whereas the plane wave basis set is chosen in the interstitial region. R_{MT} is chosen in such a way that there is no charge leakage from the core and total energy convergence is ensured. The R_{MT} is equal to 2.45, 2.45, 2.17, and 2.3 atomic unit (au) for Mn, Cd, S, and Se, respectively. The maximum value of angular momentum $\mathbf{l}_{max} = 8$ is taken for the wave function expansion inside the atomic spheres. In order to accomplish the energy eigenvalue convergence, the wave function in the interstitial region is expanded in terms of plane waves with a cutoff of $K_{max}R_{MT} = 8$. Total energy convergence is ensured using different values of the plane wave cutoff as well as the number of **k** points. We used 30 **k** points in the irreducible wedge of the Brillouin zone for the supercell calculations, and the self-consistent calculations are considered to converge only when the calculated total energy of the crystal converges to less than 0.0001 Ry.

All DMSs calculations are executed with eight atoms per supercell, raised by taking $1 \times 1 \times 1$ standard unit cell of zinc-

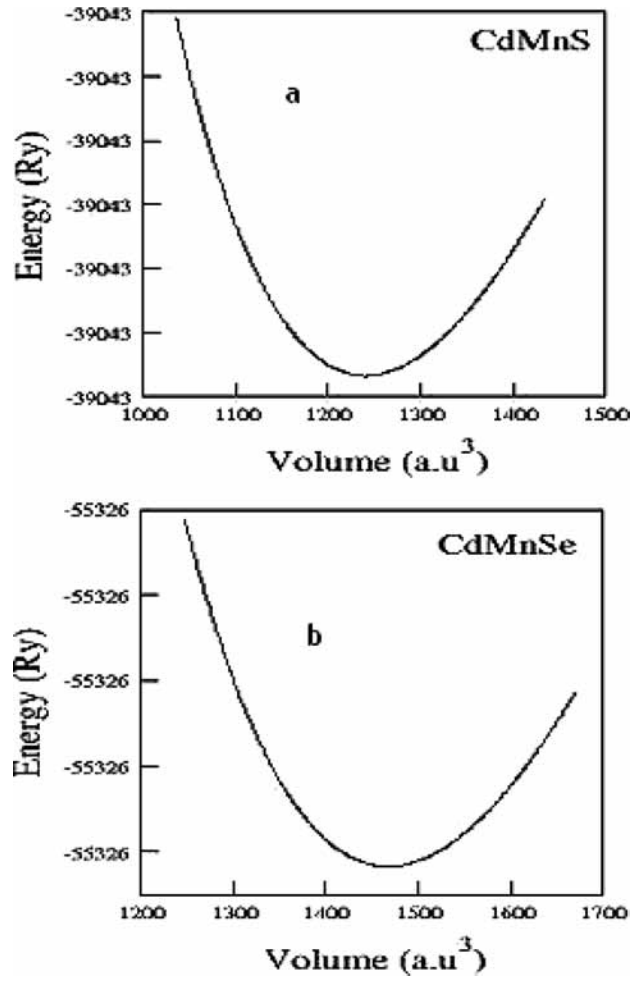

Figure 1. Variation of the total energy versus volumes for (a) $Cd_{0.75}Mn_{0.25}S$ and (b) $Cd_{0.75}Mn_{0.25}Se$.

TABLE 1: Calculated Structural Parameters for $Cd_{1-x}Mn_xS$ and $Cd_{1-x}Mn_xSe$ with 25% Mn

compound	calculations	a (Å)	B (GPa)	B'
CdS	this work	5.78	74.8811	5.0
	experimental	5.818[a]	64.4[b]	
	other calculations	5.815[c]	62.3[c]	5.466[c]
CdMnS	this work	5.68	69.4785	4.3545
CdSe	this work	6.088	56.792	5.0
	experimental	6.0840[d]		
	other calculations	6.055[c]	54.6[c]	5.57[c]
CdMnSe	this work	6.0148	53.6378	4.31
	other calculations	6.3282[e]		

[a] Reference 20. [b] Reference 21. [c] Reference 22. [d] Reference 23. [e] Reference 24.

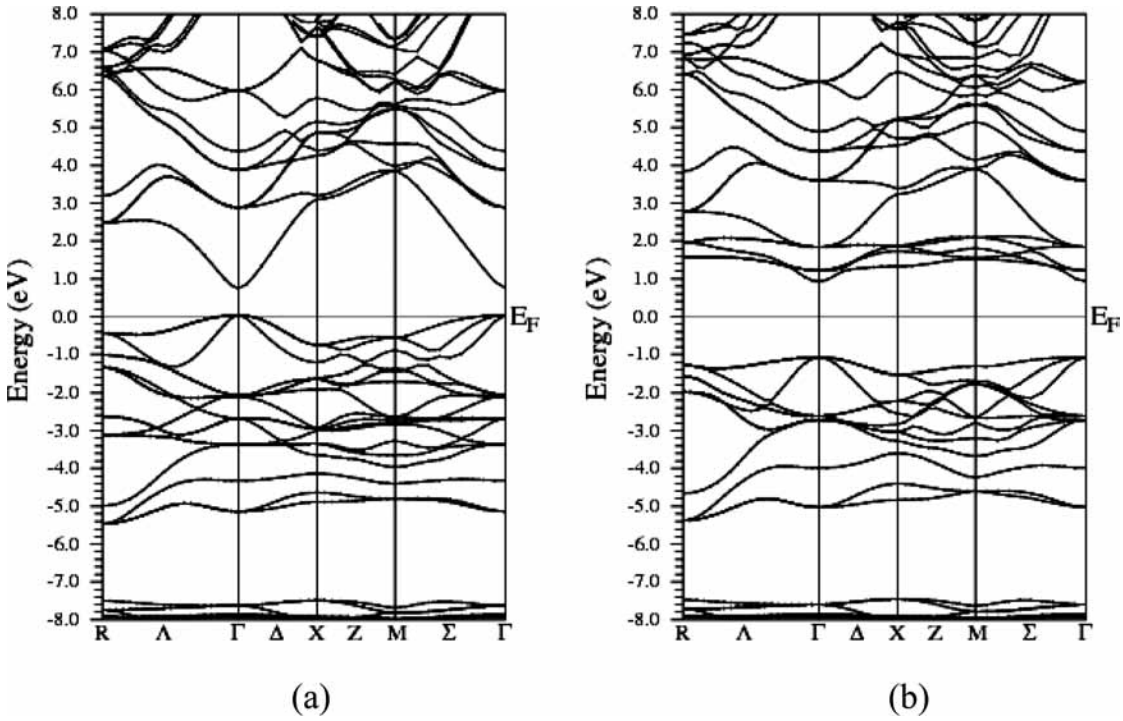

Figure 2. Electronic band structure of ferromagnetic $Cd_{0.75}Mn_{0.25}S$ for (a) spin-up and (b) spin-down structures.

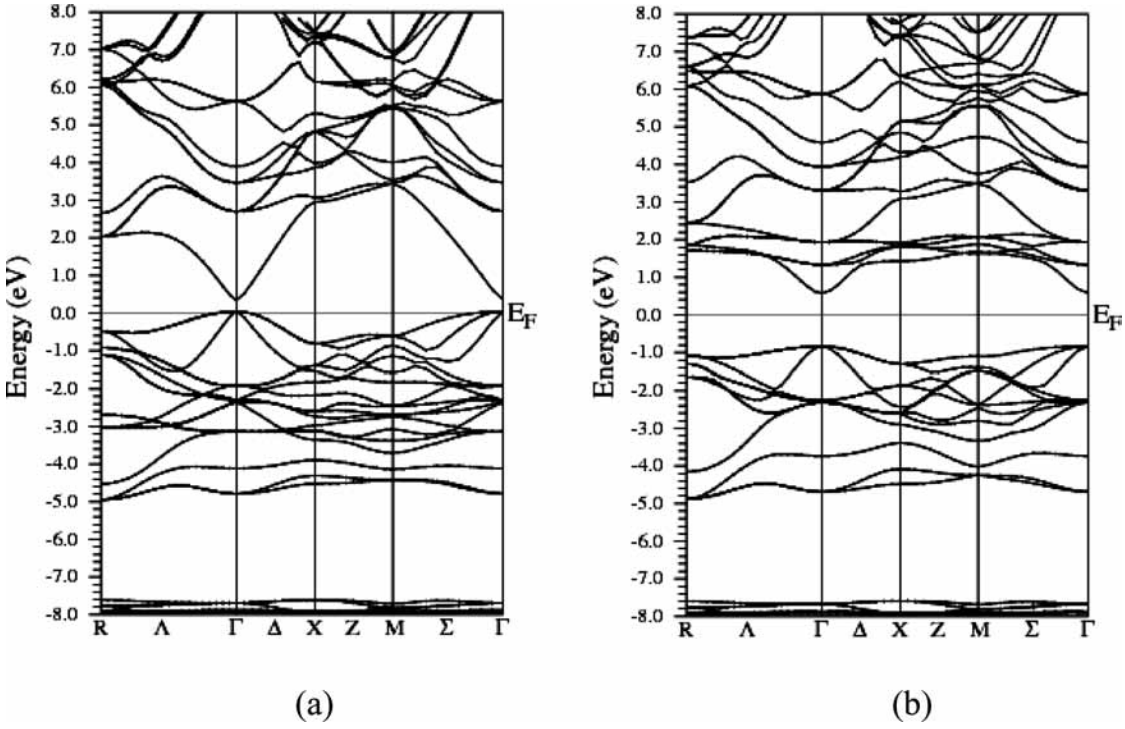

Figure 3. Electronic band structure of ferromagnetic $Cd_{0.75}Mn_{0.25}Se$ for (a) spin-up and (b) spin-down structures.

blende phase with cubic symmetry. These materials are composed of a cation sublattice where we substitute one Cd atom with a Mn atom in the supercell, getting DMSs with 25% Mn ions. As the supercell contains only one Mn atom and the infinite crystal is constructed by exact imitation of this supercell, all Mn atoms have the same neighboring atoms and possess the same spin. As a result, the $Cd_{0.75}Mn_{0.25}S$ and $Cd_{0.75}Mn_{0.25}Se$ phases are ferromagnetic.

Results and Discussion

3.1. Structural Properties. In order to study the ground-state properties of $Cd_{1-x}Mn_xS$ and $Cd_{1-x}Mn_xSe$ in the B3 phase with 25% Mn, structural optimization is performed by minimizing the total energy with respect to the unit cell volume using Murnaghan's equation of state as shown in Figure 1. The calculated equilibrium lattice constant a, the bulk modulus B, and the derivative of bulk modulus B' of the DMSs are listed in Table 1. To the best of our knowledge, there are no experimental data and theoretical calculations that have appeared in the literature yet. Therefore, we compare the results of our binary compounds CdS and CdSe with the experimental data and previous theoretical calculations (Table 1).

3.2. Electronic Band Structures and Density of States. The calculated spin-polarized band structures of $Cd_{0.75}Mn_{0.25}S$ and

TABLE 2: Energy Gaps (eV) at High-Symmetry Points from the Spin-Up Band Structure for the $Cd_{1-x}Mn_xS$ and $Cd_{1-x}Mn_xSe$ with 25% Mn

band gaps	CdMnS	CdMnSe
$E_g^{\Gamma-\Gamma}$	0.75	0.38, 0.19[a]
$E_g^{\Gamma-X}$	3.1	2.9
$E_g^{\Gamma-R}$	2.05	2.0

[a] Reference 24.

$Cd_{0.75}Mn_{0.25}Se$ for spin-up and spin-down alignments in the B3 phase are shown in Figures 2 and 3, respectively, which are drawn along the high-symmetry directions in the first Brillouin zone. Figures 2 and 3 show that both the top of the valence band and the bottom of the conduction band are located at the Γ point of the Brillouin zone, in agreement with the pure CdS and CdSe band structures. We have taken the zero of the energy scale at the top of the valence band for the spin-up case. One can observe that both $Cd_{0.75}Mn_{0.25}S$ and $Cd_{0.75}Mn_{0.25}Se$ have a direct band gap at the Γ point. The calculated values of $E_g^{\Gamma-\Gamma}$, $E_g^{\Gamma-X}$, and $E_g^{\Gamma-R}$ from spin-up band structures are listed in Table 2.

Our calculated results of total and partial density of states for $Cd_{0.75}Mn_{0.25}S$ and $Cd_{0.75}Mn_{0.25}Se$ are displayed in Figures 4 and 5, which provide a qualitative explanation of the atomic and orbital origins of different band states. We observe that in $Cd_{0.75}Mn_{0.25}S/Cd_{0.75}Mn_{0.25}Se$, the s state of S/Se along with a small contribution of the Cd p state occupies the lowest part of the valence band. The upper part of the valence band is occupied by the Cd 4d state, while close to the Fermi surface, the S/Se p states have a small contribution. The significance of the role played by Mn 3d states can be seen in the upper part of the valence band, where for the spin-up case these states are at the Fermi surface and for the spin-down case they are a few electronvolts below the Fermi surface. Above the Fermi surface, the bottom of the conduction band is dominated by Cd s states for the spin-up structure and there is a contribution of Cd s and Mn d states for the spin-down case. From Figures 4 and 5, one can also observe that the Mn 3d bands are occupied and centered at $E_v^{\uparrow} = -3.54$ eV for CdMnS and $E_v^{\uparrow} = -3.23$ eV for CdMnSe, while the spin-down Mn 3d bands are empty and centered at $E_v^{\downarrow} = +2.01$ eV for CdMnS and $E_v^{\downarrow} = +2.15$ eV for CdMnSe, where $E_v^{\uparrow}$ and $E_v^{\downarrow}$ are valence band maxima for spin-up and spin-down cases, respectively.

The spin-exchange splitting energy defined as the separation between the corresponding spin-up and spin-down peaks due to the effective Mn 3d states, $\Delta_x(d) = E(C_d^{\downarrow}) - E(C_d^{\uparrow})$, is +4.32 eV for $Cd_{0.75}Mn_{0.25}S$ and +4.14 eV for $Cd_{0.75}Mn_{0.25}Se$. We can specify the nature of attraction in these DMSs from the p−d exchange splitting $\Delta_x^v(pd) = E_v^{\downarrow} - E_v^{\uparrow}$, $\Delta_x^c(pd) = E_c^{\downarrow} - E_c^{\uparrow}$. The value of $\Delta_x^v(pd)$ and $\Delta_x^c(pd)$ for $Cd_{0.75}Mn_{0.25}S/Cd_{0.75}Mn_{0.25}Se$ are −1.53/−1.08 eV and 0.21/0.32, respectively, which shows that the effective potential for the minority spin is attractive as compared to the majority spin as in the spin-polarized system.[25]

3.3. Exchange Coupling. The significant parameters determining the magnetic properties of DMSs are the s−d exchange

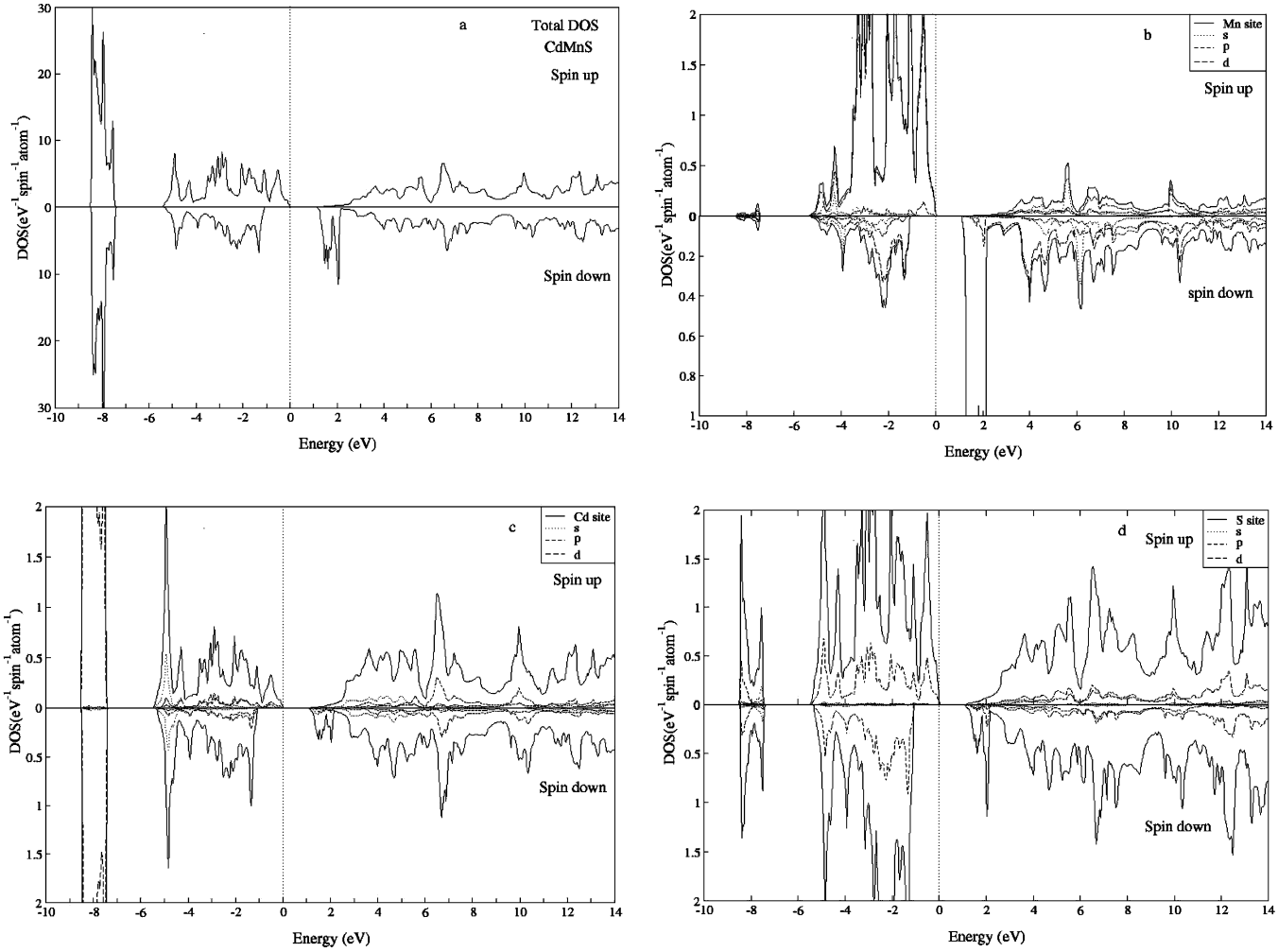

Figure 4. Total and partial local spin DOS in the B3 phase: (a) total $Cd_{0.75}Mn_{0.25}S$, (b) Mn site, (c) Cd site, and (d) S site.

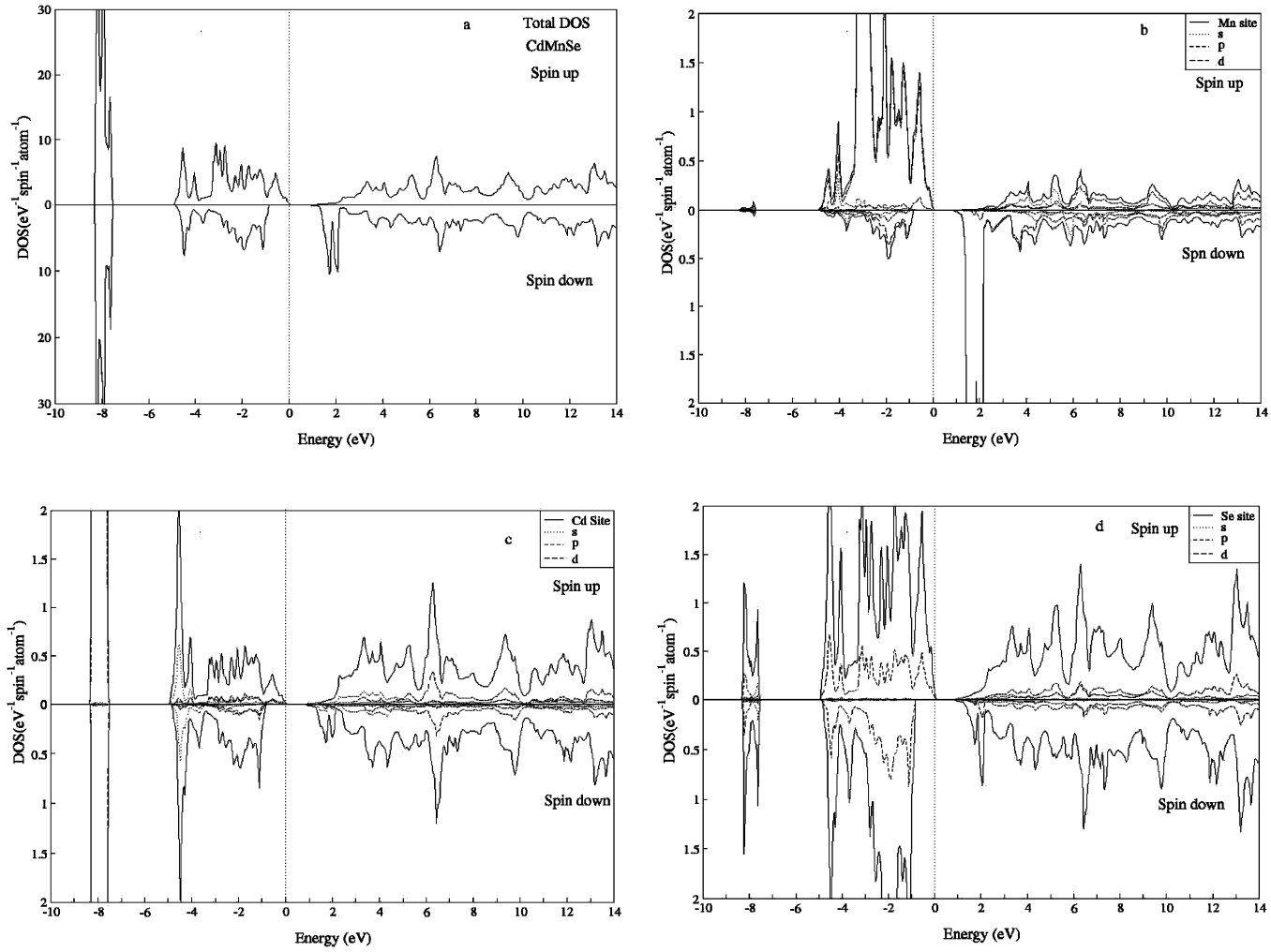

Figure 5. Total and partial local spin DOS in the B3 phase: (a) total $Cd_{0.75}Mn_{0.25}Se$, (b) Mn site, (c) Cd site, and (d) Se site.

constant $N_0\alpha$ and the p−d exchange constant $N_0\beta$, where N_0 is the concentration of cations. $N_0\alpha$ describes the exchange interactions between the conduction electron carriers and the Mn spin, whereas $N_0\beta$ explains the exchange interaction between the holes and the Mn d state. These parameters describe how the valence and conduction bands contribute in the process of exchange and splitting. From the conduction and valence band edges spin splitting ($\Delta E_c = E_c^{\downarrow} - E_c^{\uparrow}$, $\Delta E_v = E_v^{\downarrow} - E_v^{\uparrow}$), the exchange constants can be calculated directly as[26]

$$N_0\alpha = \frac{\Delta E_c}{x\langle S\rangle}, \quad N_0\beta = \frac{\Delta E_v}{x\langle S\rangle} \tag{1}$$

where x is the concentration of Mn. ΔE_c and ΔE_v are the band edge spin splittings of the conduction band maxima (CBM) and valence band maxima (VBM) at the Γ point, and $\langle S\rangle$ is one-half of the magnetization per manganese ion. Experimentally, the exchange constants are measured from the exciton band that is spin split in the optical-magnetoabsorption experiment.[27] We calculated $N_0\alpha$ and $N_0\beta$ for CdMnS and CdMnSe by using the predicted values of ΔE_c, ΔE_v, and $\langle S\rangle$, and the results are listed in Table 3. These results show that the exchange coupling between the conduction band of Cd, S, Se, and Mn impurity is ferromagnetic, which confirms the expected magnetic character of these materials.

3.4. Magnetic Properties. Our calculated results for total and local magnetic moments for DMSs CdMnS and CdMnSe in the B3 phase within the muffin-tin spheres as well as in the interstitial sites are listed in Table 4. These calculations show that the total magnetic moment of 3d electrons within the Mn sphere in CdMnS and CdMnSe are around 5.0020 and 5.00013 μ_B, respectively (i.e., the atomic arrangement of Mn is well matched with both $3d^4$ and $3d^5$). Because of the partially occupied Mn 3d levels, permanent local magnetic moments are

TABLE 3: Calculated Conduction and Valence Band Edge Spin Splitting and Exchange Constants (in eV) for the $Cd_{1-x}Mn_xS$ and $Cd_{1-x}Mn_xSe$ with 25% Mn

Compounds		ΔE_c	ΔE_v	$N_0\alpha$	$N_0\beta$
CdMnS	this work	0.21	−1.53	0.336	−2.448
	experimental			0.22[b]	−1.80[b]
CdMnSe	this work	0.32	−1.08	0.512	−1.728
	experimental			0.26[c]	−1.31[c]

[a] Reference 28. [b] Reference 29. [c] References 30−33.

TABLE 4: Calculated Magnetic Moments (in μ_B) of Several Sites and the Total Magnetic Moment for the $Cd_{1-x}Mn_xS$ and $Cd_{1-x}Mn_xSe$ with 25% Mn

site	CdMnS	CdMnSe
Mn	4.29842	4.30812, 4.32[a]
Cd	0.02401	0.02030, 0.03[a]
S	0.05066	
Se		0.02973, 0.06[a]
interstitial site	0.42716	0.41763
total μ_B	5.0020	5.00013, 5.0[a]

[a] Reference 24.

produced in DMSs. Other interesting properties of DMSs occur from the exchange relations between the magnetic ions and the electrons or holes near the band edges.[25] We can also observe that the free space charge value 5.0 μ_B of Mn reduces to 4.29842 μ_B for CdMnS and 4.30812 μ_B for CdMnSe due to p−d hybridization. Further, Mn atoms induce a local magnetic moment in Cd, S, and Se atoms, while the magnetic moments of all atoms are parallel in these DMSs materials: this could be considered as a tunneling of spin-up impurity states to neighboring atoms.[34]

Conclusions

In this paper we present the spin-polarized structural, electronic, and magnetic properties of the DMSs CdMnS and CdMnSe at 25% Mn concentration. The calculations are performed on the basis of full potential linearized augmented plane wave plus local orbital (FP-L/APW+lo) method within the spin-polarized density functional theory and the local spin density approximation (LSDA). The Mn 3d half-filled electrons have been treated as valence electrons. It is observed that due to Mn 3d hybridization both materials have well-defined spin-up and spin-down band structures. The comprehensive examination of the local densities of states has permitted us to find the exchange splitting and crystal field splitting produced by Mn 3d states. Our calculations show that the effective potential for the minority spin is more attractive than that for the majority spin as is typical in spin-polarized systems. The exchange constants $N_0\alpha$ and $N_0\beta$ have also been calculated, and the results of total and local magnetic moments indicate that Mn impurity adds no hole carriers to the perfect CdS and CdSe compounds. It is found that the magnetic moments of all atoms are parallel, while the spin-polarized charge around the Mn atom is localized. Because of the partially filled Mn 3d levels, the local magnetic moment of Mn reduces from its free space charge value due to p−d hybridization and produces small local magnetic moments on the nonmagnetic Cd, S, and Se sites.

References and Notes

(1) Galazka, R. R. *Inst. Phys. Conf. Ser.* **1979**, *43*, 133.
(2) Gaj, J. A. *J. Phys. Soc. Jpn., Suppl. A* **1980**, *49*, 797.
(3) Furdyna, J. K. *J. Appl. Phys.* **1988**, *64*, 4.
(4) Loss, D.; DiVincenzo, D. P. *Phys. Rev. A* **1998**, *57*, 120.
(5) Fiederling, R.; Keim, M.; Reuscher, G.; Ossau, W.; Schmidt, G.; Waag, A.; Molenkamp, L. W. *Nature (London)* **1999**, *402*, 790.
(6) Ohno, Y.; Young, D. K.; Beschoten, B.; Matsukura, F.; Ohno, H.; Awschalom, D. D. *Nature (London)* **1999**, *402*, 790.
(7) Koshihara, S.; Oiwa, A.; Hirasawa, M.; Katsumoto, S.; Iye, Y.; Urano, C.; Takagi, H.; Munekata, H. *Phys. Rev. Lett.* **1997**, *78*, 4617.
(8) Ohno, H.; Chiba, D.; Matsukura, F.; Omiya, T.; Abe, E.; Dietl, T.; Ohno, Y.; Ohtani, K. *Nature (London)* **2000**, *408*, 944.
(9) Dietl, T.; Ohno, H.; Matsukura, F.; Cibert, J.; Ferrand, D. *Science* **2000**, *287*, 1019.
(10) Ferrand, D.; Gibert, J.; Wasiela, A.; Bourgognon, C.; Tatarenko, S.; Fishman, G.; Andrearczyk, T.; Jaroszynski, J.; Kolesnik, S.; Dietl, T.; Barbara, B.; Dufeu, D. *Phys. Rev. B* **2001**, *63*, 85201.
(11) Taniguchi, M.; Fujimori, M.; Fujisawa, M.; Mori, T.; Souma, I.; Oka, Y. *Solid State Commun.* **1985**, *62*, 431.
(12) Wall, A.; Chang, S.; Philip, P.; Caprile, C.; Franciosi, A.; Reifenberger, R.; Pool, F. *J. Vac. Sci. Technol. A* **1987**, *5*, 2051.
(13) Mecabih, S.; Benguerine, K.; Benosman, N.; Abbar, B.; Bouhafa, B. *Physica B* **2008**, *403*, 3452.
(14) Weidemann, R.; Burmester, B.; Gumlich, H. E.; Jung, C. H.; Kleemann, T.; Kreitler, T.; Krost, A.; Middelmann, H. U.; Becker, U.; Kupsch, M.; Bernstoff, S. *J. Cryst. Growth* **1990**, *101*, 916.
(15) Chen, C.; Qu, M.; Hu, W.; Zhang, X.; Lin, F.; Hu, H. *J. Appl. Phys.* **1991**, *69*, 6114.
(16) Iacomia, F.; Salaorua, I.; Apetroaeia, N.; Vasileb, A.; Teodorescuc, C. M.; Macovei, D. *J. Optoelectron. Adv. Mater.* **2006**, *8*, 266.
(17) Karande, V. S.; Mane, S. H.; Pujari, V. B.; Deshmukh, L. P. *Turk. J. Phys.* **2003**, *27*, 559.
(18) Idrish Miah, M.; Kityk, I. V.; Mac, E.; Gray, A. *Acta Mater.* **2007**, *55*, 6392.
(19) Blaha, P.; Schwarz, K.; Madsen, G. K. H.; Kvanicka, D.; Luitz, J. *WIEN2K, An Augmented Plane Wave + Local Orbital Program for Calculating Crystal Properties*; Karlheinz Schwarz, Techn. Universitat: Wien, Austria, 2001; ISBN: 3-9501031-1-1-2.
(20) Cook, W. R., Jr. *J. Am. Ceram. Soc.* **1968**, *51*, 518.
(21) Bechstedt, F.; Harrisob, W. A. *Phys. Rev. B* **1989**, *39*, 5041.
(22) Benkabou, F.; Aourag, H.; Certier, M. *Mater. Chem. Phys.* **2000**, *66*, 10.
(23) Abrikosov, N. K.; Bankina, V. B.; Portskaya, L. V.; Shelimova, L. E.; Skudnova, E. V. *Semiconducting II-VI, IV-VI and V-VI compounds*; Plenum: New York, 1969.
(24) Zhang, C.-W.; Yan, S.-S.; Qang, P.-J.; Zhang, Z. *Comput. Mater. Sci.* **2008**, *43*, 710.
(25) Morozzi, V. L.; Janak, J. F.; Willians, A. R. *Calculated Electronic Propertied of Metals*; Pergamon: New York, 1978.
(26) Gaj, J. A.; Planel, R.; Fishman, G. *Solid State Commum.* **1984**, *29*, 861.
(27) Szczytko, J.; Mac, W.; Twardowski, A.; Matsukura, F.; Ohno, H. *Phys. Rev. B* **1999**, *59*, 12935.
(28) Heiman, D.; Shapira, Y.; Foner, S. *Solid State Commun.* **1983**, *45*, 899.
(29) Nawrocki, M.; Lascaray, J. P.; Coquillat, D.; Demi- aniuk, M. In *Proceedings of the MRS symposium on Diluted Magnetic (Semimagnetic) Semiconductors*, Boston, 1986; Aggarwal, R. L., Furdyna, J. K., von Molnar, S., Eds.; Material Research Society: Boston, 1987; Vol. 65.
(30) Heiman, D.; Shapira, Y.; Foner, S. *Solid State Commun.* **1984**, *51*, 603.
(31) Tawaardowski, A.; Dietl, T.; Demianiuk, M. *Solid State Commun.* **1983**, *48*, 845.
(32) Shapira, Y.; Heiman, D.; Foner, S. *Solid State Commun.* **1982**, *44*, 1243.
(33) Aggarwal, R. L.; Jasperson, S. N.; Stankiewicz, J.; Shapira, Y.; Foner, S.; Khazai, B.; Wold, A. *Phys. Rev. B* **1983**, *28*, 6907.
(34) Jain, M.; Kronik, L.; Chelikowsky, J. R.; Godlevsky, V. V. *Phys. Rev. B* **2001**, *64*, 245205.

JP900698Q